

**VYSE QUARRY EXTENSION,
PHASE 1 SOIL AREA,
NEAR GEORGEHAM,
DEVON.**

NGR: 249430.141519 (centred)

ARCHAEOLOGICAL INVESTIGATION

December 2019
Report No. 1334



ARCHAEOLOGICAL CONSULTANCY, MANAGEMENT & FIELD SERVICES

**VYSE QUARRY EXTENSION,
PHASE 1 SOIL AREA,
NEAR GEORGEHAM,
DEVON.**

NGR: 249430.141519 (centred)

ARCHAEOLOGICAL INVESTIGATION



**December 2019
Report No. 1334**

Quality Assurance

This Document has been compiled and authorised in accordance with AMS's Quality Procedures (ISO 9001: 2015)

Author: A. Hood BSc MCIFA

Date: 9th December 2019

Approved: R. King BA MCIFA

QA Checked: T. Michaels BSc MCIFA

This report has been compiled with all reasonable skill care and attention to detail within the terms of the project as specified by the client and within the general terms and conditions of Archaeological Management Services Ltd trading as Foundations Archaeology, but no explicit warranty is provided for information and opinions stated. AMS Ltd accepts no responsibility whatsoever to third parties to whom this report or any part thereof is made known. Any such party relies on this report at their own risk. Copyright of this document is retained by AMS Ltd, but unlimited licence to reproduce it in whole or part is granted to the client and/or their agents and/or assignees on payment of invoice.

Vyse Quarry Extension, Phase 1 Soil Area, Near Georgeham, Devon: Archaeological Investigation

CONTENTS

Summary

Glossary of Archaeological Terms and Abbreviations

- 1 INTRODUCTION
- 2 PROJECT BACKGROUND
- 3 AIMS
- 4 METHODOLOGY
- 5 RESULTS
- 6 DISCUSSION
- 7 CONCLUSION
- 8 BIBLIOGRAPHY
- 9 ACKNOWLEDGEMENTS

APPENDICES

Appendix 1: Stratigraphic Data

Appendix 2: Report on the Optical Dating of Sediments

Vyse Quarry Extension, Phase 1 Soil Area, Near Georgeham, Devon: Archaeological Investigation

FIGURE LIST

- Figure 1: Site Location
- Figure 2: Site Plan
- Figure 3: Excavated Features in Relation to Earthwork
- Figure 4: Trench 11 Plan and Section
- Figure 5: Trench 12 Plan and Section
- Figure 6: Trench 13 Plan and Section
- Figure 7: Earthwork in Relation to Terrain
- Figure 8: Earthwork in Relation to 1888 OS Map
- Figure 9: Earthwork in Relation to 1905 OS Map
- Figure 10: Earthwork in Relation to 1963 OS Map
- Figure 11: Photographs

Vyse Quarry Extension, Phase 1 Soil Area, Near Georgeham, Devon: Archaeological Investigation

SUMMARY

Between 23rd April and 1st May 2019 Foundations Archaeology undertook an archaeological investigation on land at Vyse Quarry, Near Georgeham, Devon (NGR: 249430.141519 - centred). The project was commissioned by Andrew Josephs Associates on behalf of Braunton Aggregates.

The fieldwork comprised the archaeological excavation and recording of three trenches, which were targeted upon a previously identified linear earthwork.

The investigation established that the earthwork feature comprised part of a double-ditch boundary, which could be tentatively dated to the later Iron Age or Roman period, based upon a single Optically Stimulated Luminescence (OSL) date. The function of the boundary remained uncertain; however, it was possible that it was originally constructed in order to at least partially enclose a south facing landscape spur. There were no associated features or finds within the investigation trenches.

GLOSSARY OF ARCHAEOLOGICAL TERMS AND ABBREVIATIONS

Archaeology

For the purpose of this project, archaeology is taken to mean the study of past human societies through their material remains from prehistoric times to the modern era. No rigid upper date limit has been set, but AD 1900 is used as a general cut-off point.

CBM

Ceramic Building Material.

Natural

In archaeological terms this refers to the undisturbed natural geology of a site.

NGR

National Grid Reference from the Ordnance Survey Grid.

OD

Ordnance datum; used to express a given height above sea-level. (AOD Above Ordnance Datum).

OS

Ordnance Survey.

OSL

(Optically Stimulated Luminescence) A technique used to date the last time a quartz sediment was exposed to light.

Prehistoric

The period prior to the Roman invasion of AD 43, traditionally sub divided into; *Palaeolithic* – c. 500,000 BC to c. 12,000 BC; *Mesolithic* – c. 12,000 BC to c. 4,500 BC; *Neolithic* – c. 4,500 BC to c. 2,000 BC; *Bronze Age* – c. 2,000 BC to c. 800 BC; *Iron Age* – c. 800 BC to AD 43.

Roman

The period traditionally dated AD 43 until AD 410.

1 INTRODUCTION

- 1.1 This report presents the findings of an archaeological investigation undertaken by Foundations Archaeology between 23rd April and 1st May 2019 on land at Vyse Quarry, Near Georgeham, Devon (NGR: 249430.141519 - centred). The project was commissioned by Andrew Josephs Associates on behalf of Braunton Aggregates.
- 1.2 The investigation was conducted in accordance with the approved Written Scheme of Investigation (WSI), prepared by Foundations Archaeology (2019b) and the Chartered Institute for Archaeologists (CIfA) *Standards and Guidance for Archaeological Excavation* (2014).
- 1.3 The code of conduct of the CIfA was adhered to throughout.

2 PROJECT BACKGROUND

- 2.1 The site is located within agricultural fields, approximately 1.6km to the northeast of North Buckland, at the north of Vyse Quarry. The study area is located on the upper, southwest facing slopes of a spur, between approximately 175m AOD at the north and 160m AOD at the south. The underlying geology is recorded as *Pickwell Down Sandstones Formation* - sandstone (BGS Online Viewer).
- 2.2 The archaeological works were undertaken in response to a proposed 4ha extension to the northeast and southeast of Vyse Quarry. In accordance with the principles of NPPF18, the Senior Historic Environment Officer for Devon County Council requested archaeological investigations in order to attempt to date and elucidate the form and function of a double-ditched earthwork feature, which had previously been the focus of a geophysical survey (TigerGeo Ltd. 2018) and subsequent evaluation (Foundations Archaeology 2018).
- 2.3 The site is within an area of archaeological potential. A search of the Historic Environment Record for the area produced 21 entries, which were predominately of Post-medieval date. No entries which predated the Medieval period were present, although the site of Spreacombe Manor (MDV 14512) and pond (MDV 31685) may have Medieval or earlier origins. Evidence of previous industrial activity in the form of adits, mines (MDV 245, 246, 19500, 54868) and quarrying (MDV 31600 and 31681) is present across the study area. Evidence of World War II activity is fairly extensive across the landscape, in the form of assault practice areas (MDV 73990).
- 2.4 The earliest historic map available for the area is the Tithe Map dated 1839. The quarry and proposed southern extension are contained within North Down (land parcel 367), which was described as a 'Furze Brake'. This rough grass condition appeared to continue through the first half of the twentieth century, with the area depicted as bracken, heath or rough grassland on the 1888, 1905

Vyse Quarry Extension, Phase 1 Soil Area, Near Georgeham, Devon: Archaeological Investigation

and 1963 OS maps. However, the northern extension area only partly extends into the area of rough ground, with the rest of the site shown as clear and was therefore most likely pasture or under arable. Vyse Quarry first appears on the 1958 OS map and clearly expanded over the subsequent decades. Up to the 1963 mapping, the broader landscape and land divisions appear relatively unchanged since the late 19th century, apart from the areas of rough grassland, which seem to be more limited, possibly due to land improvements by drainage.

- 2.5 A geophysical survey, undertaken within the site, revealed a series of former field systems and probable ditches (TigerGeo Ltd. 2018).
- 2.6 A total of ten evaluation trenches were excavated across the site by Foundations Archaeology in 2018. The results of this work identified a generally low potential for archaeological remains within the study area. However, a substantial double-ditch earthwork feature was present at the north of the site, which was thought to be related to known World War II training activity in the vicinity. This feature was investigated by Trench 1, but remained undated.
- 2.7 Subsequent to the archaeological evaluation, the double-ditch feature was subjected to an earthwork survey (Foundations Archaeology 2019a).
- 2.8 The site therefore contained the potential for evidence of predominately Medieval and WWII activity, as well as the undated earthwork. This did not prejudice the works against the recovery of data relating to other periods.

3 AIMS

- 3.1 The aims of the archaeological investigation were to make an appropriate record of the archaeological deposits affected by the quarry extension. The archaeological works comprised the excavation of a series of investigation trenches across the undated earthwork feature. A specific objective was to recover datable material/artefacts, in order to help to understand the nature and significance of the heritage asset.

4 METHODOLOGY

- 4.1 A total of three archaeological investigation trenches (Trenches 11 – 13) were excavated within the site, as shown in Figures 2 and 3. The trenches were located to provide a broadly representative sample of the double-ditched earthwork.
- 4.2 Non-significant overburden was removed, under constant archaeological supervision, to the top of the archaeological remains or the underlying natural deposits, whichever was encountered first. This was achieved through the use

of a mechanical excavator, equipped with a toothless grading bucket. Features and spoil tips were visually scanned for finds.

- 4.3 Sections were manually excavated across all of the ditches present within the investigation trenches. All excavation and recording work was undertaken in accordance with the WSI and the Foundations Archaeology Technical Manual 3: Excavation Manual. The initial excavation of features failed to yield artefacts and it was therefore agreed on site that the features present within Trench 12 were to be excavated to a 100% sample level.

5 RESULTS

- 5.1 A full description of all contexts identified during the course of the evaluation is presented in Appendix 1. A summary of the results is given below.
- 5.2 The general stratigraphic sequence within the site was relatively uniform across the investigated areas. Natural silt sand was present at an average depth of 0.27m below the Modern ground. This was overlaid by a silt sand topsoil, average 0.27m thick. A layer of sand silt (1302), up to 0.15m thick, which was present in the southern part of Trench 13, possibly represented part of a remnant subsoil or, more likely, the degraded/weathered top of natural deposits. Where features were present, they were cut into the top of the natural substrates. Visibility conditions were generally good and there was no direct evidence for significant truncation or Modern disturbance within the trenches.
- 5.3 The curvilinear earthwork measured approximately 160m in length and was situated on a northeast – southwest alignment. The limited investigation indicated that it consisted of at least two parallel ditches, although, the earthwork survey suggested that the feature was potentially more complex at the north, beyond the development boundary, where three possible ditches were present. The western ditch ([1109]/[1207]) was up to 3.41m wide and 0.32m in depth. This was separated from the eastern ditch by a berm, up to 3 - 4m in width. The eastern ditch ([1102]/[1202/11]/[1303]) was up to 4.10m wide and 0.70m in depth. Both of the ditches had sloping edges, with rounded to flat basal profiles. Ditch [1202] had possibly been re-cut [1211] after a period of initial silting; however, this interpretation was somewhat tentative. The eastern ditch was very shallow in Trench 13, which suggested that it terminated or dissipated at that location. The ditches contained numerous silt sand soil fills, which were completely devoid of artefactual material. There was a general paucity of charcoal within the ditch fills, although some charcoal flecks and lenses of charcoal were noted in fill (1105), within ditch [1102]. There was no convincing evidence for any associated banks or other features.
- 5.4 A sediment sample (VYSE01), obtained from fill (1103), near to the base of ditch [1102], was subjected to Optically Stimulated Luminescence (OSL) analysis, which yielded a calendrical date range of 120 BC to AD 270, at the 1 sigma confidence level (Appendix 2; Toms 2019).

6 DISCUSSION

- 6.1 The archaeological investigation has indicated that the earthwork represented the in-filled remains of a possible later Iron Age or Roman double-ditch boundary feature. However, the date of the feature is based upon a single OSL determination, at the 1 sigma confidence level, and, as such, should be regarded as tentative. Due to the limited nature of the investigation it was not possible to confidently suggest the original extent of the ditches and, as such, their function remained uncertain. However, their curvilinear form and relationship to the surrounding topography suggested the possibility that they were intended to at least partially enclose a south facing landscape spur (Figure 7).

7 CONCLUSION

- 7.1 The archaeological investigations at Vyse Quarry have provided a tentative later Iron Age to Roman date for a double-ditch boundary, which may have formed part of an enclosure. There were no associated features or finds within the investigated areas and, as such, the precise nature and function of the possible enclosure remains uncertain.
- 7.2 The archive is currently held at the offices of Foundations Archaeology, but will be deposited in due course with the Museum of Barnstable and North Devon. A short note will be submitted for publication in the relevant local archaeological journal and an OASIS form will also be submitted to ADS.

8 BIBLIOGRAPHY

Chartered Institute for Archaeologists. 2014. *Standard and Guidance for Archaeological Excavation*. Reading.

Foundations Archaeology. 2018. *Vyse Quarry Extension, Near Georgeham, Devon: Archaeological Evaluation*. Unpublished.

Foundations Archaeology. 2019a. *Vyse Quarry Extension, Near Georgeham, Devon: Archaeological Earthwork Survey*. Unpublished.

Foundations Archaeology. 2019b. *Vyse Quarry Extension, Phase 1 Soil Area, Near Georgeham, Devon: Written Scheme of Investigation for a Staged Programme of Archaeological Investigation*. Unpublished.

TigerGeo Ltd. 2018. *Land at Vyse Quarry, Near Georgeham, Devon: Archaeological Geophysical Survey*. Unpublished.

Vyse Quarry Extension, Phase 1 Soil Area, Near Georgeham, Devon: Archaeological Investigation

Toms, P. 2019. *Optical Dating of Sediments: Vyse Quarry excavations, UK*. University of Gloucestershire: Luminescence Dating Laboratory. Unpublished.

9 ACKNOWLEDGEMENTS

Foundations Archaeology would like to thank Stephen Reed of Devon County Council, along with Andy Josephs and Ian Meadows of Andrew Josephs Associates and the staff at Braunton Aggregates for their help during the course of the project.

Wyse Quarry Extension, Phase 1 Soil Area, Near Georgeham, Devon: Archaeological Investigation

APPENDIX 1: Stratigraphic Data

| CXT | L(m) | W(m) | D(m) | DESCRIPTION | CUTS/LATER THAN | CUT BY/EARLIER THAN |
|--------|-------|------|------|--|-----------------|---------------------|
| | | | | Trench 11: 15.70m long by 2.40m wide. Natural = orange brown to pink brown silt sand, which contained occasional small angular stones. Present at average depth of 0.20m (165.17m AOD) below Modern ground. | | |
| 1101 | 15.70 | 2.40 | 0.20 | Topsoil: grey brown silt sand. | 1107, 1110 | n/a |
| [1102] | 2.40 | 4.10 | 0.70 | Northeast – southwest aligned ditch with sloping sides and a flat base. Contained fills 1103 – 1108. | natural | 1103 |
| 1103 | ? | 1.30 | 0.22 | Fill of ditch [1102]: light grey brown silt sand, which contained occasional small stones. | [1102] | 1104 |
| 1104 | ? | 0.90 | 0.17 | Fill of ditch [1102]: dark orange brown silt sand. | 1103 | 1105 |
| 1105 | ? | 3.25 | 0.37 | Fill of ditch [1102]: mid to dark brown silt clay sand, which contained occasional flecks and lenses of charcoal. | 1104 | 1106 |
| 1106 | ? | 3.90 | 0.30 | Fill of ditch [1102]: dark brown silt clay sand, which contained occasional stones. | 1105 | 1108 |
| 1107 | ? | 1.05 | 0.17 | Fill of ditch [1102]: bright orange brown silt clay sand, which contained occasional stones. | 1108 | 1101 |
| 1108 | ? | 1.40 | 0.19 | Fill of ditch [1102]: mid grey brown silt clay sand, which contained occasional stones. | 1106 | 1107 |
| [1109] | 2.37 | 3.41 | 0.32 | Northeast – southwest aligned ditch with a shallow, flat profile. Contained fill 1110. | natural | 1110 |
| 1110 | 2.37 | 3.41 | 0.32 | Fill of ditch [1109]: dark brown silt clay sand, which contained occasional stones. | [1109] | 1101 |
| | | | | Trench 12: 15.35m long by 2.40m wide. Natural = orange brown to pink brown silt sand, which contained occasional small angular stones. Present at average depth of 0.25m (162.51m AOD) below Modern ground. | | |
| 1201 | 15.35 | 2.40 | 0.25 | Topsoil: grey brown silt sand. | 1203, 1208 | n/a |
| [1202] | ? | 3.20 | 0.30 | Northeast – southwest aligned ditch with a rounded profile. Contained fills 1210, 1206 and 1205. | natural | 1210 |
| 1203 | ? | 0.95 | 0.15 | Fill of ditch [1211]: mid brown pink silt sand, which contained occasional angular stones. | 1204 | 1201 |
| 1204 | ? | 3.95 | 0.32 | Fill of ditch [1211]: dark brown silt sand, which contained occasional stones. | 1212 | 1203 |
| 1205 | ? | 2.40 | 0.13 | Fill of ditch [1202]: light brown silt sand, which contained occasional stones. | 1206 | [1211] |
| 1206 | ? | 1.57 | 0.07 | Fill of ditch [1202]: light brown grey silt sand, which contained occasional small stones. | 1210 | 1205 |
| [1207] | 2.50 | 2.55 | 0.20 | Northeast – southwest aligned ditch with a shallow, flat profile. Contained fills 1209 and 1208. | natural | 1209 |
| 1208 | ? | 2.40 | 0.15 | Fill of ditch [1207]: dark brown silt clay, which contained frequent stones. | 1209 | 1201 |
| 1209 | ? | 2.20 | 0.05 | Fill of ditch [1207]: light grey brown silt sand, which contained occasional small stones. | [1207] | 1208 |
| 1210 | ? | 3.20 | 0.13 | Fill of ditch [1202]: mid brown orange silt sand, which contained occasional small stones. | [1202] | 1206 |
| [1211] | 2.90 | 3.90 | 0.32 | Possible re-cut of ditch [1202] with a wide, rounded profile. Contained fills 1212 and 1204. | 1205 | 1212 |
| 1212 | ? | 2.55 | 0.03 | Fill of ditch [1211]: brown silt sand, which contained frequent small stones. | [1211] | 1204 |

Vyse Quarry Extension, Phase 1 Soil Area, Near Georgeham, Devon: Archaeological Investigation

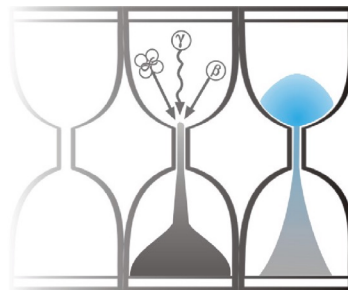
| CXT | L(m) | W(m) | D(m) | DESCRIPTION | CUTS/LATER THAN | CUT BY/EARLIER THAN |
|--------|-------|------|------|---|-----------------|---------------------|
| | | | | Trench 13: 14.20m long by 2.40m wide. Natural = orange brown silt sand, which contained occasional small angular stones. Present at average depth of 0.35m (161.22m AOD) below Modern ground. | | |
| 1301 | 14.20 | 2.40 | 0.35 | Topsoil: brown silt sand. | 1302, 1304 | n/a |
| 1302 | ? | 2.35 | 0.15 | Layer of light brown sand silt, which contained rare charcoal flecks. Present at the southwest end of the trench; dissipated to the northeast. Possible subsoil or degraded/disturbed top of natural. | natural | 1301 |
| [1303] | 2.80 | 2.0 | 0.08 | North – south aligned ditch with a shallow, flat profile. Contained fill 1304. | natural | 1304 |
| 1304 | 2.80 | 2.0 | 0.08 | Fill of ditch [1303]: grey brown silt clay, which contained occasional small stones and rare charcoal flecks. | [1303] | 1301 |

APPENDIX 2: Report on the Optical Dating of Sediments



University of Gloucestershire

Luminescence dating laboratory



Optical dating of sediments: Vyse Quarry excavations, UK

to

S. Reed

Historic Environment Team, Devon County Council

Sample Collection, Analysis & Reporting, Prof. P.S. Toms

Sample Preparation & Measurement, Mr J.C. Wood

10 July 2019

Contents

| Section | | Page |
|---------|---|------|
| | Table 1 D_r , D_e and Age data of submitted samples | 3 |
| | Table 2 Analytical validity of sample suite ages | 4 |
| 1.0 | Mechanisms and Principles | 5 |
| 2.0 | Sample Collection and Preparation | 5 |
| 3.0 | Acquisition and accuracy of D_e value | 6 |
| | 3.1 Laboratory Factors | 6 |
| | 3.1.1 Feldspar Contamination | 6 |
| | 3.1.2 Preheating | 6 |
| | 3.1.3 Irradiation | 7 |
| | 3.1.4 Internal Consistency | 7 |
| | 3.2 Environmental Factors | 7 |
| | 3.2.1 Incomplete Zeroing | 7 |
| | 3.2.2 Turbation | 8 |
| 4.0 | Acquisition and accuracy of D_r value | 8 |
| 5.0 | Estimation of age | 9 |
| 6.0 | Analytical Uncertainty | 9 |
| | Sample diagnostics, luminescence and age data | 12 |
| | References | 13 |

Scope of Report

This is a standard report of the Luminescence dating laboratory, University of Gloucestershire. In large part, the document summarises the processes, diagnostics and data drawn upon to deliver Table 1. A conclusion on the analytical validity of each sample's optical age estimate is expressed in Table 2; where there are caveats, the reader is directed to the relevant section of the report that explains the issue further in general terms.

Copyright Notice

Permission must be sought from Prof. P.S. Toms of the University of Gloucestershire Luminescence dating laboratory in using the content of this report, in part or whole, for the purpose of publication.

| Field Code | Lab Code | Overburden (m) | Grain size (μm) | Moisture content (%) | NaI γ -spectrometry (<i>in situ</i>) γ D _r (Gy.ka ⁻¹) | Ge γ -spectrometry (<i>ex situ</i>) | | | β D _r (Gy.ka ⁻¹) | Cosmic D _r (Gy.ka ⁻¹) | Preheat (°C for 10s) | Low Dose Repeat Ratio | Interpolated:Applied Low Regenerative-dose D _e | High Dose Repeat Ratio | Interpolated:Applied High Regenerative-dose D _e | Post-IR OSL Ratio |
|------------|----------|----------------|------------------------------|----------------------|--|--|-------------|-------------|--|---|-------------------------|-----------------------|---|------------------------|--|-------------------|
| | | | | | | K (%) | Th (ppm) | U (ppm) | | | | | | | | |
| VYSE01 | GL18107 | 0.86 | 125-180 | 19 ± 5 | 0.82 ± 0.10 | 1.35 ± 0.09 | 9.66 ± 0.59 | 2.20 ± 0.15 | 1.15 ± 0.14 | 0.19 ± 0.02 | 260 | 1.02 ± 0.04 | 1.02 ± 0.03 | 1.00 ± 0.02 | 1.01 ± 0.02 | 1.01 ± 0.04 |

| Field Code | Lab Code | Total D _r (Gy.ka ⁻¹) | D _e (Gy) | Age (ka) | Date |
|------------|----------|--|------------------------|--------------------|---------------------|
| VYSE01 | GL18107 | 2.16 ± 0.19 | 4.2 ± 0.2 | 1.94 ± 0.19 (0.17) | 120 B.C. – 270 A.D. |

Table 1 D_r, D_e and Age data of submitted samples located at c. 51°N, 4°W, 165m. Age estimates expressed relative to year of sampling. Uncertainties in age are quoted at 1 σ confidence, are based on analytical errors and reflect combined systematic and experimental variability and (in parenthesis) experimental variability alone (see 6.0). **Blue** indicates samples with accepted age estimates, **red**, age estimates with caveats (see Table 2).

| Generic considerations | Field Code | Lab Code | Sample specific considerations |
|------------------------|------------|----------|--------------------------------|
| None | VYSE01 | GL18107 | None |

Table 2 Analytical validity of sample suite age estimates and caveats for consideration

1.0 Mechanisms and principles

Upon exposure to ionising radiation, electrons within the crystal lattice of insulating minerals are displaced from their atomic orbits. Whilst this dislocation is momentary for most electrons, a portion of charge is redistributed to meta-stable sites (traps) within the crystal lattice. In the absence of significant optical and thermal stimuli, this charge can be stored for extensive periods. The quantity of charge relocation and storage relates to the magnitude and period of irradiation. When the lattice is optically or thermally stimulated, charge is evicted from traps and may return to a vacant orbit position (hole). Upon recombination with a hole, an electron's energy can be dissipated in the form of light generating crystal luminescence providing a measure of dose absorption.

Herein, quartz is segregated for dating. The utility of this minerogenic dosimeter lies in the stability of its datable signal over the mid to late Quaternary period, predicted through isothermal decay studies (e.g. Smith *et al.*, 1990; retention lifetime 630 Ma at 20°C) and evidenced by optical age estimates concordant with independent chronological controls (e.g. Murray and Olley, 2002). This stability is in contrast to the anomalous fading of comparable signals commonly observed for other ubiquitous sedimentary minerals such as feldspar and zircon (Wintle, 1973; Templer, 1985; Spooner, 1993)

Optical age estimates of sedimentation (Huntley *et al.*, 1985) are premised upon reduction of the minerogenic time dependent signal (Optically Stimulated Luminescence, OSL) to zero through exposure to sunlight and, once buried, signal reformulation by absorption of litho- and cosmogenic radiation. The signal accumulated post burial acts as a dosimeter recording total dose absorption, converting to a chronometer by estimating the rate of dose absorption quantified through the assay of radioactivity in the surrounding lithology and streaming from the cosmos.

$$\text{Age} = \frac{\text{Mean Equivalent Dose (D}_e\text{, Gy)}}{\text{Mean Dose Rate (D}_r\text{, Gy.ka}^{-1}\text{)}}$$

Aitken (1998) and Bøtter-Jensen *et al.* (2003) offer a detailed review of optical dating.

2.0 Sample Collection and Preparation

One sediment sample was collected within opaque tubing and submitted for Optical dating. To preclude optical erosion of the datable signal prior to measurement, all samples were opened and prepared under controlled laboratory illumination provided by Encapsulite RB-10 (red) filters. To isolate that material potentially exposed to daylight during sampling, sediment located within 20 mm of each tube-end was removed.

The remaining sample was dried and then sieved. The fine sand fraction was segregated and subjected to acid and alkaline digestion (10% HCl, 15% H₂O₂) to attain removal of carbonate and organic components respectively. A further acid digestion in HF (40%, 60 mins) was used to etch the outer 10-15 µm layer affected by α radiation and degrade each samples' feldspar content. During HF treatment, continuous magnetic stirring was used to effect isotropic etching of grains. 10% HCl was then added to remove acid soluble fluorides. Each sample was dried, resieved and quartz isolated from the remaining heavy mineral fraction using a sodium polytungstate density separation at 2.68g.cm⁻³. Twelve 8 mm multi-grain aliquots (c. 3-6 mg) of quartz from each sample were then mounted on aluminium discs for determination of D_e values.

All drying was conducted at 40°C to prevent thermal erosion of the signal. All acids and alkalis were Analar grade. All dilutions (removing toxic-corrosive and non-minerogenic luminescence-bearing substances) were conducted with distilled water to prevent signal contamination by extraneous particles.

3.0 Acquisition and accuracy of D_e value

All minerals naturally exhibit marked inter-sample variability in luminescence per unit dose (sensitivity). Therefore, the estimation of D_e acquired since burial requires calibration of the natural signal using known amounts of laboratory dose. D_e values were quantified using a single-aliquot regenerative-dose (SAR) protocol (Murray and Wintle 2000; 2003) facilitated by a Risø TL-DA-15 irradiation-stimulation-detection system (Markey *et al.*, 1997; Bøtter-Jensen *et al.*, 1999). Within this apparatus, optical signal stimulation is provided by an assembly of blue diodes (5 packs of 6 Nichia NSPB500S), filtered to 470 ± 80 nm conveying $15 \text{ mW}\cdot\text{cm}^{-2}$ using a 3 mm Schott GG420 positioned in front of each diode pack. Infrared (IR) stimulation, provided by 6 IR diodes (Telefunken TSHA 6203) stimulating at 875 ± 80 nm delivering $\sim 5 \text{ mW}\cdot\text{cm}^{-2}$, was used to indicate the presence of contaminant feldspars (Hütt *et al.*, 1988). Stimulated photon emissions from quartz aliquots are in the ultraviolet (UV) range and were filtered from stimulating photons by 7.5 mm HOYA U-340 glass and detected by an EMI 9235QA photomultiplier fitted with a blue-green sensitive bialkali photocathode. Aliquot irradiation was conducted using a $1.48 \text{ GBq } ^{90}\text{Sr}/^{90}\text{Y } \beta$ source calibrated for multi-grain aliquots of $125\text{-}180 \mu\text{m}$ quartz against the 'Hotspot 800' $^{60}\text{Co } \gamma$ source located at the National Physical Laboratory (NPL), UK.

SAR by definition evaluates D_e through measuring the natural signal (Fig. 1) of a single aliquot and then regenerating that aliquot's signal by using known laboratory doses to enable calibration. For each aliquot, five different regenerative-doses were administered so as to image dose response. D_e values for each aliquot were then interpolated, and associated counting and fitting errors calculated, by way of exponential plus linear regression (Fig. 1). Weighted (geometric) mean D_e values were calculated from 12 aliquots using the central age model outlined by Galbraith *et al.* (1999) and are quoted at 1σ confidence (Table 1). The accuracy with which D_e equates to total absorbed dose and that dose absorbed since burial was assessed. The former can be considered a function of laboratory factors, the latter, one of environmental issues. Diagnostics were deployed to estimate the influence of these factors and criteria instituted to optimise the accuracy of D_e values.

3.1 Laboratory Factors

3.1.1 Feldspar contamination

The propensity of feldspar signals to fade and underestimate age, coupled with their higher sensitivity relative to quartz makes it imperative to quantify feldspar contamination. At room temperature, feldspars generate a signal (IRSL; Fig. 1) upon exposure to IR whereas quartz does not. The signal from feldspars contributing to OSL can be depleted by prior exposure to IR. For all aliquots the contribution of any remaining feldspars was estimated from the OSL IR depletion ratio (Duller, 2003). The influence of IR depletion on the OSL signal can be illustrated by comparing the regenerated post-IR OSL D_e with the applied regenerative-dose. If the addition to OSL by feldspars is insignificant, then the repeat dose ratio of OSL to post-IR OSL should be statistically consistent with unity (Table 1). If any aliquots do not fulfil this criterion, then the sample age estimate should be accepted tentatively. The source of feldspar contamination is rarely rooted in sample preparation; it predominantly results from the occurrence of feldspars as inclusions within quartz.

3.1.2 Preheating

Preheating aliquots between irradiation and optical stimulation is necessary to ensure comparability between natural and laboratory-induced signals. However, the multiple irradiation and preheating steps that are required to define single-aliquot regenerative-dose response leads to signal sensitisation, rendering calibration of the natural signal inaccurate. The SAR protocol (Murray and Wintle, 2000; 2003) enables this sensitisation to be monitored and corrected using a test dose, here set at 5 Gy preheated to 220°C for 10s, to track signal sensitivity between irradiation-preheat steps. However, the accuracy of sensitisation correction for both natural and laboratory signals can be preheat dependent.

The Dose Recovery test was used to assess the optimal preheat temperature for accurate correction and calibration of the time dependent signal. Dose Recovery (Fig. 2) attempts to quantify the combined effects of thermal transfer and

sensitisation on the natural signal, using a precise lab dose to simulate natural dose. The ratio between the applied dose and recovered D_e value should be statistically concordant with unity. For this diagnostic, 6 aliquots were each assigned a 10 s preheat between 180°C and 280°C.

That preheat treatment fulfilling the criterion of accuracy within the Dose Recovery test was selected to generate the final D_e value from a further 12 aliquots. Further thermal treatments, prescribed by Murray and Wintle (2000; 2003), were applied to optimise accuracy and precision. Optical stimulation occurred at 125°C in order to minimise effects associated with photo-transferred thermoluminescence and maximise signal to noise ratios. Inter-cycle optical stimulation was conducted at 280°C to minimise recuperation.

3.1.3 Irradiation

For all samples having D_e values in excess of 100 Gy, matters of signal saturation and laboratory irradiation effects are of concern. With regards the former, the rate of signal accumulation generally adheres to a saturating exponential form and it is this that limits the precision and accuracy of D_e values for samples having absorbed large doses. For such samples, the functional range of D_e interpolation by SAR has been verified up to 600 Gy by Pawley *et al.* (2010). Age estimates based on D_e values exceeding this value should be accepted tentatively.

3.1.4 Internal consistency

Abanico plots (Dietze *et al.*, 2016) are used to illustrate inter-aliquot D_e variability (Fig. 3). D_e values are standardised relative to the central D_e value for natural signals and are described as overdispersed when >5% lie beyond $\pm 2\sigma$ of the standardising value; resulting from a heterogeneous absorption of burial dose and/or response to the SAR protocol. For multi-grain aliquots, overdispersion of natural signals does not necessarily imply inaccuracy. However where overdispersion is observed for regenerated signals, the efficacy of sensitivity correction may be problematic. Murray and Wintle (2000; 2003) suggest repeat dose ratios (Table 1) offer a measure of SAR protocol success, whereby ratios ranging across 0.9-1.1 are acceptable. However, this variation of repeat dose ratios in the high-dose region can have a significant impact on D_e interpolation. The influence of this effect can be outlined by quantifying the ratio of interpolated to applied regenerative-dose ratio (Table 1). In this study, where both the repeat dose ratios and interpolated to applied regenerative-dose ratios range across 0.9-1.1, sensitivity-correction is considered effective.

3.2 Environmental factors

3.2.1 Incomplete zeroing

Post-burial OSL signals residual of pre-burial dose absorption can result where pre-burial sunlight exposure is limited in spectrum, intensity and/or period, leading to age overestimation. This effect is particularly acute for material eroded and redeposited sub-aqueously (Olley *et al.*, 1998, 1999; Wallinga, 2002) and exposed to a burial dose of <20 Gy (e.g. Olley *et al.*, 2004), has some influence in sub-aerial contexts but is rarely of consequence where aerial transport has occurred. Within single-aliquot regenerative-dose optical dating there are two diagnostics of partial resetting (or bleaching); signal analysis (Agersnap-Larsen *et al.*, 2000; Bailey *et al.*, 2003) and inter-aliquot D_e distribution studies (Murray *et al.*, 1995).

Within this study, signal analysis was used to quantify the change in D_e value with respect to optical stimulation time for multi-grain aliquots. This exploits the existence of traps within minerogenic dosimeters that bleach with different efficiency for a given wavelength of light to verify partial bleaching. $D_e(t)$ plots (Fig. 4; Bailey *et al.*, 2003) are constructed from separate integrals of signal decay as laboratory optical stimulation progresses. A statistically significant increase in natural $D_e(t)$ is indicative of partial bleaching assuming three conditions are fulfilled. Firstly, that a statistically significant increase in $D_e(t)$ is observed when partial bleaching is simulated within the laboratory. Secondly, that there is no significant rise in $D_e(t)$ when full bleaching is simulated. Finally, there should be no significant augmentation in $D_e(t)$ when zero dose is simulated. Where partial bleaching is detected, the age derived from the sample should be considered a maximum estimate only. However, the utility of signal analysis is strongly dependent upon a samples pre-burial

experience of sunlight's spectrum and its residual to post-burial signal ratio. Given in the majority of cases, the spectral exposure history of a deposit is uncertain, the absence of an increase in natural D_e (t) does not necessarily testify to the absence of partial bleaching.

Where requested and feasible, the insensitivities of multi-grain single-aliquot signal analysis may be circumvented by inter-aliquot D_e distribution studies. This analysis uses aliquots of single sand grains to quantify inter-grain D_e distribution. At present, it is contended that asymmetric inter-grain D_e distributions are symptomatic of partial bleaching and/or pedoturbation (Murray *et al.*, 1995; Olley *et al.*, 1999; Olley *et al.*, 2004; Bateman *et al.*, 2003). For partial bleaching at least, it is further contended that the D_e acquired during burial is located in the minimum region of such ranges. The mean and breadth of this minimum region is the subject of current debate, as it is additionally influenced by heterogeneity in microdosimetry, variable inter-grain response to SAR and residual to post-burial signal ratios.

3.2.2 Turbation

As noted in section 3.1.1, the accuracy of sedimentation ages can further be controlled by post-burial trans-strata grain movements forced by pedo- or cryoturbation. Berger (2003) contends pedogenesis prompts a reduction in the apparent sedimentation age of parent material through bioturbation and illuviation of younger material from above and/or by biological recycling and resetting of the datable signal of surface material. Berger (2003) proposes that the chronological products of this remobilisation are A-horizon age estimates reflecting the cessation of pedogenic activity, Bc/C-horizon ages delimiting the maximum age for the initiation of pedogenesis with estimates obtained from Bt-horizons providing an intermediate age 'close to the age of cessation of soil development'. Singhvi *et al.* (2001), in contrast, suggest that B and C-horizons closely approximate the age of the parent material, the A-horizon, that of the 'soil forming episode'. Recent analyses of inter-aliquot D_e distributions have reinforced this complexity of interpreting burial age from pedoturbated deposits (Lombard *et al.*, 2011; Gliganic *et al.*, 2015; Jacobs *et al.*, 2008; Bateman *et al.*, 2007; Gliganic *et al.*, 2016). At present there is no definitive post-sampling mechanism for the direct detection of and correction for post-burial sediment remobilisation. However, intervals of palaeosol evolution can be delimited by a maximum age derived from parent material and a minimum age obtained from a unit overlying the palaeosol. Inaccuracy forced by cryoturbation may be bidirectional, heaving older material upwards or drawing younger material downwards into the level to be dated. Cryogenic deformation of matrix-supported material is, typically, visible; sampling of such cryogenically-disturbed sediments can be avoided.

4.0 Acquisition and accuracy of D_r value

Lithogenic D_r values were defined through measurement of U, Th and K radionuclide concentration and conversion of these quantities into β and γ D_r values (Table 1). β contributions were estimated from sub-samples by laboratory-based γ spectrometry using an Ortec GEM-S high purity Ge coaxial detector system, calibrated using certified reference materials supplied by CANMET. γ dose rates were estimated from *in situ* NaI gamma spectrometry. *In situ* measurements were conducted using an EG&G μ Nomad portable NaI gamma spectrometer (calibrated using the block standards at RLHA, University of Oxford); these reduce uncertainty relating to potential heterogeneity in the γ dose field surrounding each sample. The level of U disequilibrium was estimated by laboratory-based Ge γ spectrometry. Estimates of radionuclide concentration were converted into D_r values (Adamiec and Aitken, 1998), accounting for D_r modulation forced by grain size (Mejdahl, 1979) and present moisture content (Zimmerman, 1971). Cosmogenic D_r values were calculated on the basis of sample depth, geographical position and matrix density (Prescott and Hutton, 1994).

The spatiotemporal validity of D_r values can be considered a function of five variables. Firstly, age estimates devoid of *in situ* γ spectrometry data should be accepted tentatively if the sampled unit is heterogeneous in texture or if the sample is located within 300 mm of strata consisting of differing texture and/or mineralogy. However, where samples are obtained

throughout a vertical profile, consistent values of γD_r based solely on laboratory measurements may evidence the homogeneity of the γ field and hence accuracy of γD_r values. Secondly, disequilibrium can force temporal instability in U and Th emissions. The impact of this infrequent phenomenon (Olley *et al.*, 1996) upon age estimates is usually insignificant given their associated margins of error. However, for samples where this effect is pronounced (>50% disequilibrium between ^{238}U and ^{226}Ra ; Fig. 5), the resulting age estimates should be accepted tentatively. Thirdly, pedogenically-induced variations in matrix composition of B and C-horizons, such as radionuclide and/or mineral remobilisation, may alter the rate of energy emission and/or absorption. If D_r is invariant through a dated profile and samples encompass primary parent material, then element mobility is likely limited in effect. Fourthly, spatiotemporal detractions from present moisture content are difficult to assess directly, requiring knowledge of the magnitude and timing of differing contents. However, the maximum influence of moisture content variations can be delimited by recalculating D_r for minimum (zero) and maximum (saturation) content. Finally, temporal alteration in the thickness of overburden alters cosmic D_r values. Cosmic D_r often forms a negligible portion of total D_r . It is possible to quantify the maximum influence of overburden flux by recalculating D_r for minimum (zero) and maximum (surface sample) cosmic D_r .

5.0 Estimation of Age

Ages reported in Table 1 provide an estimate of sediment burial period based on mean D_e and D_r values and their associated analytical uncertainties. Uncertainty in age estimates is reported as a product of systematic and experimental errors, with the magnitude of experimental errors alone shown in parenthesis (Table 1). Cumulative frequency plots indicate the inter-aliquot variability in age (Fig. 6). The maximum influence of temporal variations in D_r forced by minima-maxima in moisture content and overburden thickness is also illustrated in Fig. 6. Where uncertainty in these parameters exists this age range may prove instructive, however the combined extremes represented should not be construed as preferred age estimates. The analytical validity of each sample is presented in Table 2.

6.0 Analytical uncertainty

All errors are based upon analytical uncertainty and quoted at 1σ confidence. Error calculations account for the propagation of systematic and/or experimental (random) errors associated with D_e and D_r values.

For D_e values, systematic errors are confined to laboratory β source calibration. Uncertainty in this respect is that combined from the delivery of the calibrating γ dose (1.2%; NPL, pers. comm.), the conversion of this dose for SiO_2 using the respective mass energy-absorption coefficient (2%; Hubbell, 1982) and experimental error, totalling 3.5%. Mass attenuation and bremsstrahlung losses during γ dose delivery are considered negligible. Experimental errors relate to D_e interpolation using sensitisation corrected dose responses. Natural and regenerated sensitisation corrected dose points (S_i) were quantified by,

$$S_i = (D_i - x.L_i) / (d_i - x.L_i) \quad \text{Eq.1}$$

where D_i = Natural or regenerated OSL, initial 0.2 s
 L_i = Background natural or regenerated OSL, final 5 s
 d_i = Test dose OSL, initial 0.2 s
 x = Scaling factor, 0.08

The error on each signal parameter is based on counting statistics, reflected by the square-root of measured values. The propagation of these errors within Eq. 1 generating σS_i follows the general formula given in Eq. 2. σS_i were then used to define fitting and interpolation errors within exponential plus linear regressions.

For D_r values, systematic errors accommodate uncertainty in radionuclide conversion factors (5%), β attenuation coefficients (5%), matrix density (0.20 g.cm^{-3}), vertical thickness of sampled section (specific to sample collection device), saturation moisture content (3%), moisture content attenuation (2%), burial moisture content (25% relative, unless direct evidence exists of the magnitude and period of differing content) and NaI gamma spectrometer calibration (3%). Experimental errors are associated with radionuclide quantification for each sample by NaI and Ge gamma spectrometry.

The propagation of these errors through to age calculation was quantified using the expression,

$$\sigma y (\delta y / \delta x) = (\sum ((\delta y / \delta x_n) \cdot \sigma x_n)^2)^{1/2} \quad \text{Eq. 2}$$

where y is a value equivalent to that function comprising terms x_n and where σy and σx_n are associated uncertainties.

Errors on age estimates are presented as combined systematic and experimental errors and experimental errors alone. The former (combined) error should be considered when comparing luminescence ages herein with independent chronometric controls. The latter assumes systematic errors are common to luminescence age estimates generated by means identical to those detailed herein and enable direct comparison with those estimates.

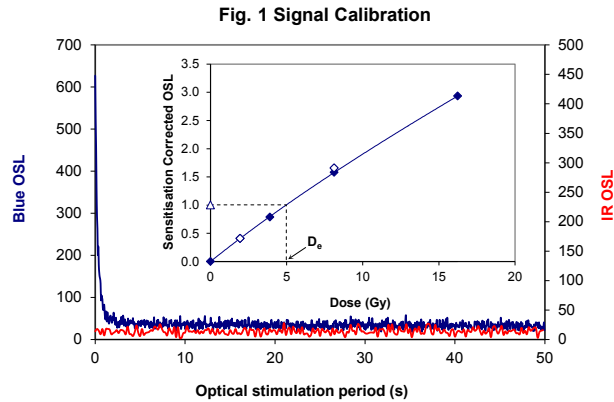


Fig. 1 Signal Calibration

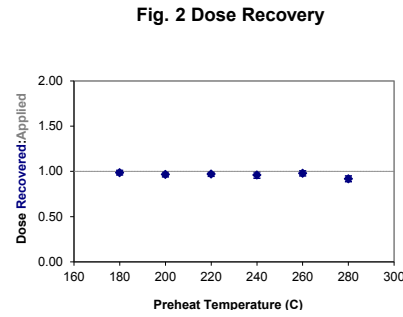


Fig. 2 Dose Recovery

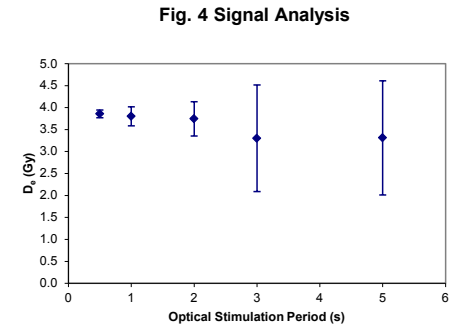


Fig. 4 Signal Analysis

Fig. 3 Inter-aliquot De distribution

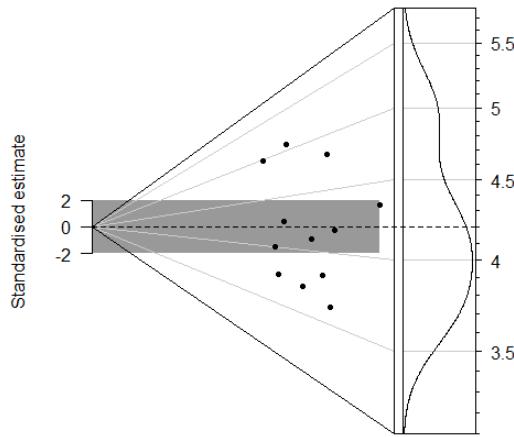


Fig. 1 Signal Calibration Natural blue and laboratory-induced infrared (IR) OSL signals. Detectable IR signal decays are diagnostic of feldspar contamination. Inset, the natural blue OSL signal (open triangle) of each aliquot is calibrated against known laboratory doses to yield equivalent dose (D_e) values. Repeats of low and high doses (open diamonds) illustrate the success of sensitivity correction.

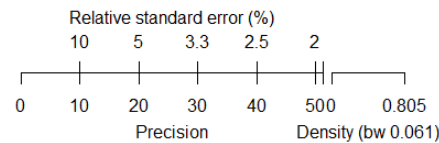
Fig. 2 Dose Recovery The acquisition of D_e values is necessarily predicated upon thermal treatment of aliquots succeeding environmental and laboratory irradiation. The Dose Recovery test quantifies the combined effects of thermal transfer and sensitisation on the natural signal using a precise lab dose to simulate natural dose. Based on this an appropriate thermal treatment is selected to generate the final D_e value.

Fig. 3 Inter-aliquot D_e distribution Abanico plot of inter-aliquot statistical concordance in D_e values derived from natural irradiation. Discordant data (those points lying beyond ± 2 standardised $\ln D_e$) reflect heterogeneous dose absorption and/or inaccuracies in calibration.

Fig. 4 Signal Analysis Statistically significant increase in natural D_e value with signal stimulation period is indicative of a partially-bleached signal, provided a significant increase in D_e results from simulated partial bleaching followed by insignificant adjustment in D_e for simulated zero and full bleach conditions. Ages from such samples are considered maximum estimates. In the absence of a significant rise in D_e with stimulation time, simulated partial bleaching and zero/full bleach tests are not assessed.

Fig. 5 U Activity Statistical concordance (equilibrium) in the activities of the daughter radioisotope ^{226}Ra with its parent ^{238}U may signify the temporal stability of D_e emissions from these chains. Significant differences (disequilibrium; $>50\%$) in activity indicate addition or removal of isotopes creating a time-dependent shift in D_e values and increased uncertainty in the accuracy of age estimates. A 20% disequilibrium marker is also shown.

Fig. 6 Age Range The Cumulative frequency plot indicates the inter-aliquot variability in age. It also shows the mean age range; an estimate of sediment burial period based on mean D_e and D_e values with associated analytical uncertainties. The maximum influence of temporal variations in D_e forced by minima-maxima variation in moisture content and overburden thickness is outlined and may prove instructive where there is uncertainty in these parameters. However the combined extremes represented should not be construed as preferred age estimates.



Sample: GL18107

Fig. 5 U Decay Activity

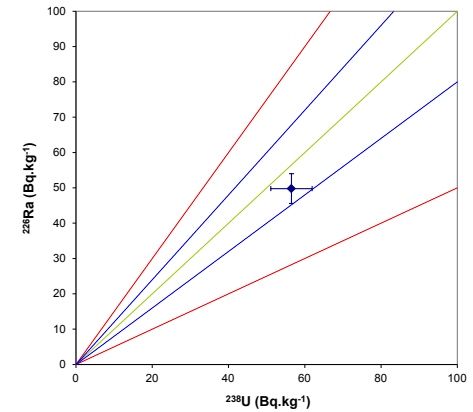
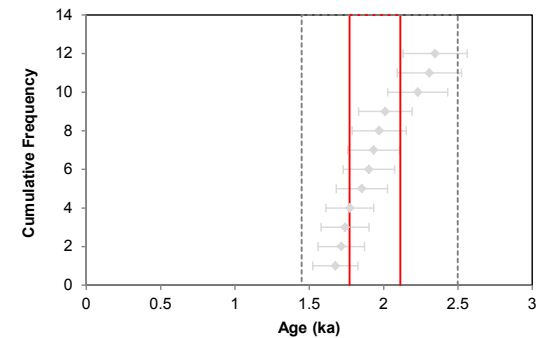


Fig. 6 Age Range



References

- Adamiec, G. and Aitken, M.J. (1998) Dose-rate conversion factors: new data. *Ancient TL*, 16, 37-50.
- Agersnap-Larsen, N., Bulur, E., Bøtter-Jensen, L. and McKeever, S.W.S. (2000) Use of the LM-OSL technique for the detection of partial bleaching in quartz. *Radiation Measurements*, 32, 419-425.
- Aitken, M. J. (1998) An introduction to optical dating: the dating of Quaternary sediments by the use of photon-stimulated luminescence. Oxford University Press.
- Bailey, R.M., Singarayer, J.S. , Ward, S. and Stokes, S. (2003) Identification of partial resetting using D_e as a function of illumination time. *Radiation Measurements*, 37, 511-518.
- Bateman, M.D., Frederick, C.D., Jaiswal, M.K., Singhvi, A.K. (2003) Investigations into the potential effects of pedoturbation on luminescence dating. *Quaternary Science Reviews*, 22, 1169-1176.
- Bateman, M.D., Boulter, C.H., Carr, A.S., Frederick, C.D., Peter, D. and Wilder, M. (2007) Detecting post-depositional sediment disturbance in sandy deposits using optical luminescence. *Quaternary Geochronology*, 2, 57-64.
- Berger, G.W. (2003). Luminescence chronology of late Pleistocene loess-paleosol and tephra sequences near Fairbanks, Alaska. *Quaternary Research*, 60, 70-83.
- Bøtter-Jensen, L., Mejdahl, V. and Murray, A.S. (1999) New light on OSL. *Quaternary Science Reviews*, 18, 303-310.
- Bøtter-Jensen, L., McKeever, S.W.S. and Wintle, A.G. (2003) *Optically Stimulated Luminescence Dosimetry*. Elsevier, Amsterdam.
- Dietze, M., Kreutzer, S., Burow, C., Fuchs, M.C., Fischer, M., Schmidt, C. (2016) The abanico plot: visualising chronometric data with individual standard errors. *Quaternary Geochronology*, 31, 1-7.
- Duller, G.A.T (2003) Distinguishing quartz and feldspar in single grain luminescence measurements. *Radiation Measurements*, 37, 161-165.
- Galbraith, R. F., Roberts, R. G., Laslett, G. M., Yoshida, H. and Olley, J. M. (1999) Optical dating of single and multiple grains of quartz from Jinmium rock shelter (northern Australia): Part I, Experimental design and statistical models. *Archaeometry*, 41, 339-364.
- Glignani, L.A., May, J.-H. and Cohen, T.J. (2015). All mixed up: using single-grain equivalent dose distributions to identify phases of pedogenic mixing on a dryland alluvial fan. *Quaternary International*, 362, 23-33.
- Glignani, L.A., Cohen, T.J., Slack, M. and Feathers, J.K. (2016) Sediment mixing in Aeolian sandsheets identified and quantified using single-grain optically stimulated luminescence. *Quaternary Geochronology*, 32, 53-66.
- Huntley, D.J., Godfrey-Smith, D.I. and Thewalt, M.L.W. (1985) Optical dating of sediments. *Nature*, 313, 105-107.
- Hubbell, J.H. (1982) Photon mass attenuation and energy-absorption coefficients from 1keV to 20MeV. *International Journal of Applied Radioisotopes*, 33, 1269-1290.

- Hütt, G., Jaek, I. and Tchonka, J. (1988) Optical dating: K-feldspars optical response stimulation spectra. *Quaternary Science Reviews*, 7, 381-386.
- Jacobs, A., Wintle, A.G., Duller, G.A.T, Roberts, R.G. and Wadley, L. (2008) New ages for the post-Howiesons Poort, late and finale middle stone age at Sibdu, South Africa. *Journal of Archaeological Science*, 35, 1790-1807.
- Lombard, M., Wadley, L., Jacobs, Z., Mohapi, M. and Roberts, R.G. (2011) Still Bay and serrated points from the Umhlatuzana rock shelter, Kwazulu-Natal, South Africa. *Journal of Archaeological Science*, 37, 1773-1784.
- Markey, B.G., Bøtter-Jensen, L., and Duller, G.A.T. (1997) A new flexible system for measuring thermally and optically stimulated luminescence. *Radiation Measurements*, 27, 83-89.
- Mejdahl, V. (1979) Thermoluminescence dating: beta-dose attenuation in quartz grains. *Archaeometry*, 21, 61-72.
- Murray, A.S. and Olley, J.M. (2002) Precision and accuracy in the Optically Stimulated Luminescence dating of sedimentary quartz: a status review. *Geochronometria*, 21, 1-16.
- Murray, A.S. and Wintle, A.G. (2000) Luminescence dating of quartz using an improved single-aliquot regenerative-dose protocol. *Radiation Measurements*, 32, 57-73.
- Murray, A.S. and Wintle, A.G. (2003) The single aliquot regenerative dose protocol: potential for improvements in reliability. *Radiation Measurements*, 37, 377-381.
- Murray, A.S., Olley, J.M. and Caitcheon, G.G. (1995) Measurement of equivalent doses in quartz from contemporary water-lain sediments using optically stimulated luminescence. *Quaternary Science Reviews*, 14, 365-371.
- Olley, J.M., Murray, A.S. and Roberts, R.G. (1996) The effects of disequilibria in the Uranium and Thorium decay chains on burial dose rates in fluvial sediments. *Quaternary Science Reviews*, 15, 751-760.
- Olley, J.M., Caitcheon, G.G. and Murray, A.S. (1998) The distribution of apparent dose as determined by optically stimulated luminescence in small aliquots of fluvial quartz: implications for dating young sediments. *Quaternary Science Reviews*, 17, 1033-1040.
- Olley, J.M., Caitcheon, G.G. and Roberts R.G. (1999) The origin of dose distributions in fluvial sediments, and the prospect of dating single grains from fluvial deposits using -optically stimulated luminescence. *Radiation Measurements*, 30, 207-217.
- Olley, J.M., Pietsch, T. and Roberts, R.G. (2004) Optical dating of Holocene sediments from a variety of geomorphic settings using single grains of quartz. *Geomorphology*, 60, 337-358.
- Pawley, S.M., Toms, P.S., Armitage, S.J., Rose, J. (2010) Quartz luminescence dating of Anglian Stage fluvial sediments: Comparison of SAR age estimates to the terrace chronology of the Middle Thames valley, UK. *Quaternary Geochronology*, 5, 569-582.
- Prescott, J.R. and Hutton, J.T. (1994) Cosmic ray contributions to dose rates for luminescence and ESR dating: large depths and long-term time variations. *Radiation Measurements*, 23, 497-500.

Singhvi, A.K., Bluszcz, A., Bateman, M.D., Someshwar Rao, M. (2001). Luminescence dating of loess-palaeosol sequences and coversands: methodological aspects and palaeoclimatic implications. *Earth Science Reviews*, 54, 193-211.

Smith, B.W., Rhodes, E.J., Stokes, S., Spooner, N.A. (1990) The optical dating of sediments using quartz. *Radiation Protection Dosimetry*, 34, 75-78.

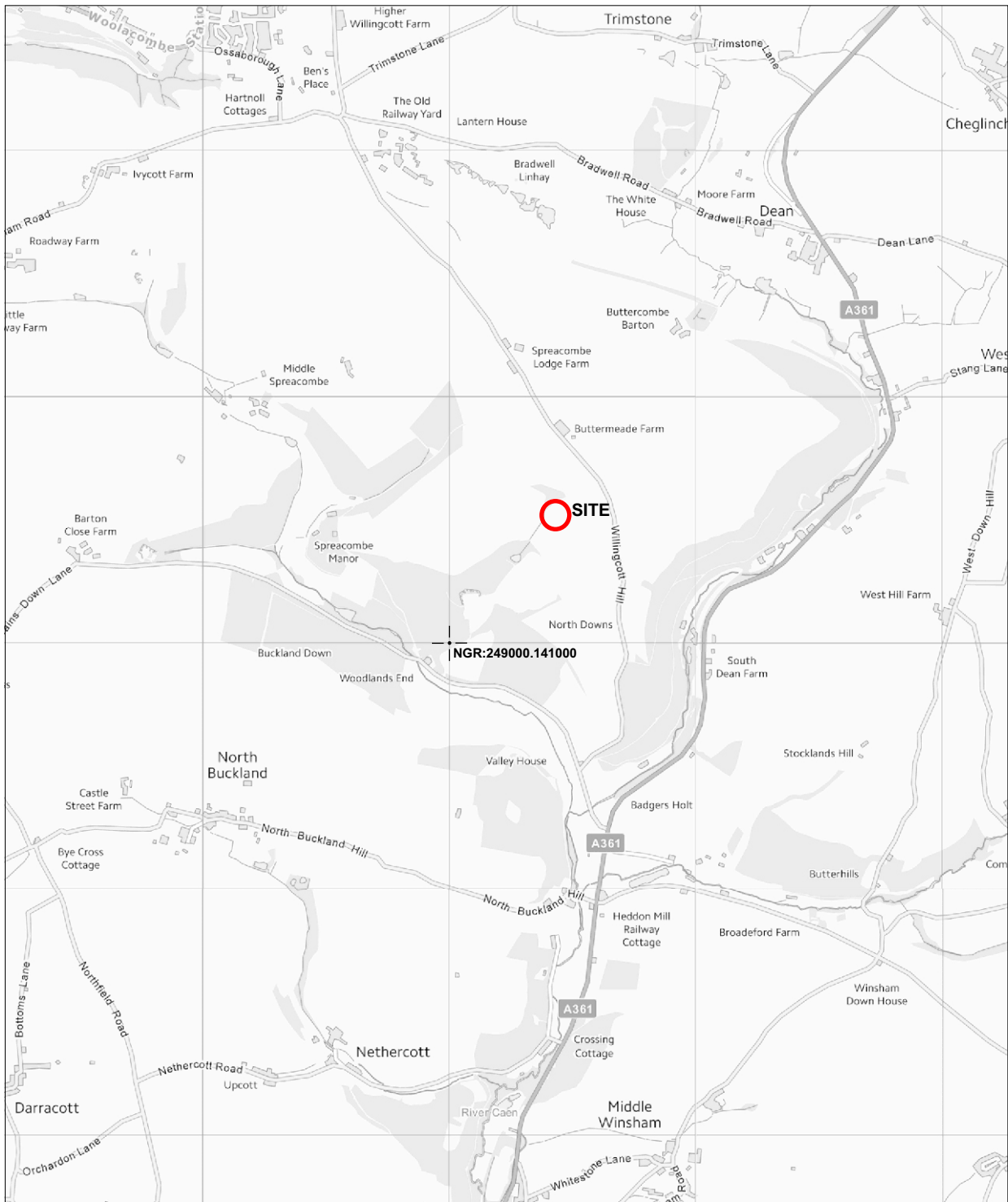
Spooner, N.A. (1993) The validity of optical dating based on feldspar. Unpublished D.Phil. thesis, Oxford University.

Templer, R.H. (1985) The removal of anomalous fading in zircons. *Nuclear Tracks and Radiation Measurements*, 10, 531-537.

Wallinga, J. (2002) Optically stimulated luminescence dating of fluvial deposits: a review. *Boreas* 31, 303-322.

Wintle, A.G. (1973) Anomalous fading of thermoluminescence in mineral samples. *Nature*, 245, 143-144.

Zimmerman, D. W. (1971) Thermoluminescent dating using fine grains from pottery. *Archaeometry*, 13, 29-52.

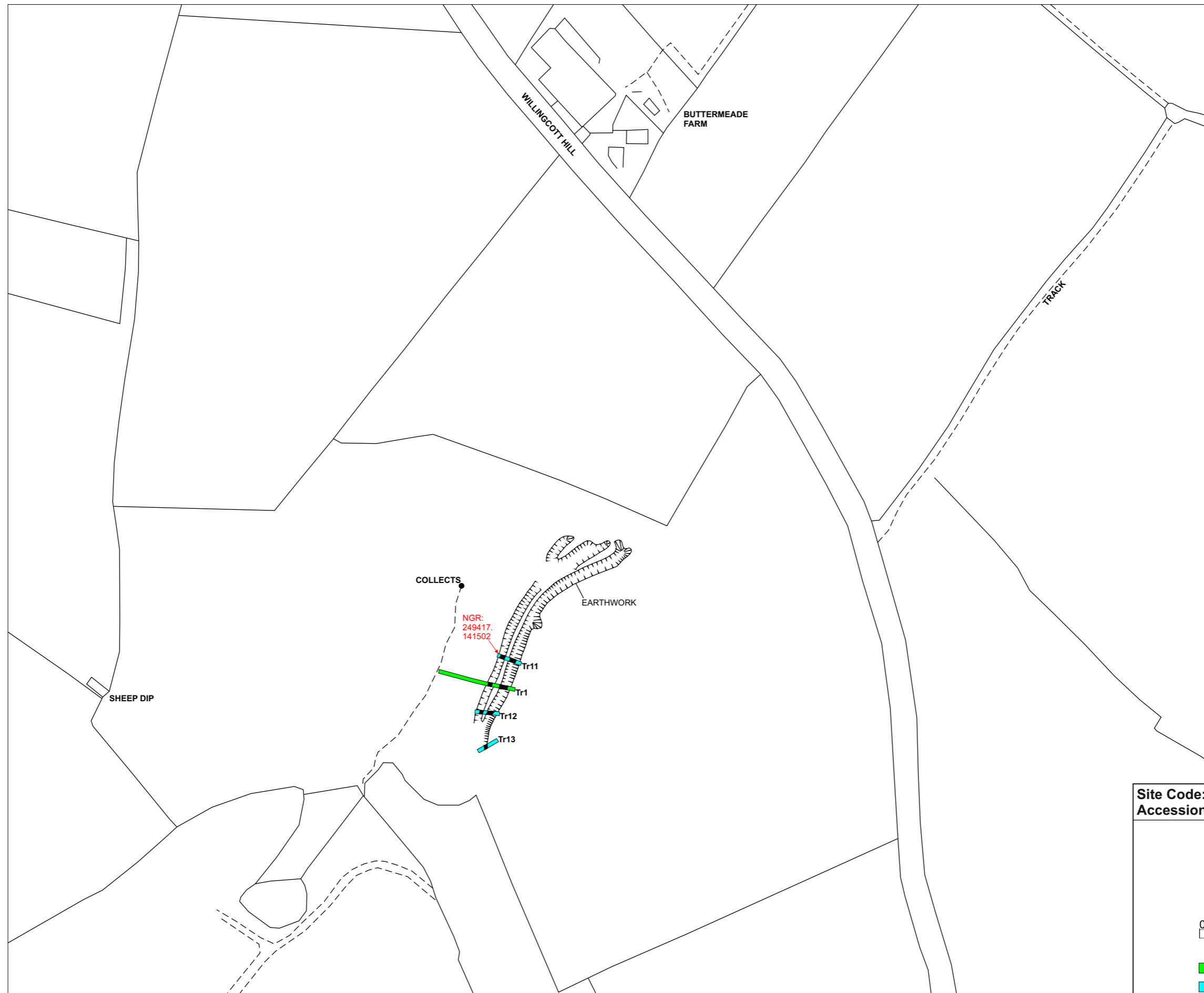


© Crown Copyright and Database Right 2019.
 Ordnance Survey Licence 100015722

Site Code: VQE19
Accession Code:

0m 1km

FIGURE 1: Site Location



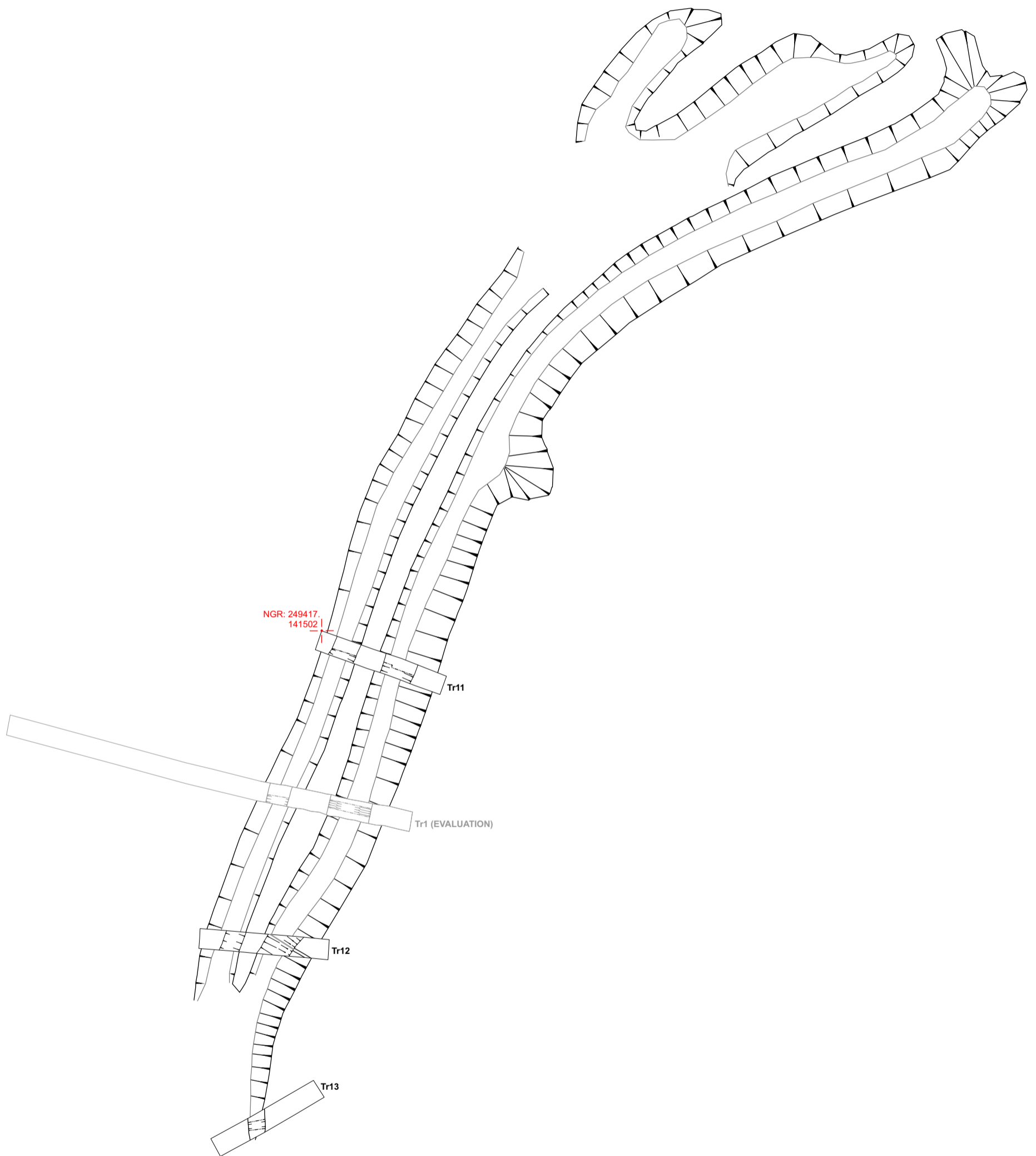
Site Code: VQE19
Accession Code:

N

0m 100m

█ = EVALUATION TRENCH
█ = INVESTIGATION TRENCH
█ = DITCH FEATURE WITHIN TRENCH

FIGURE 2: Site Plan

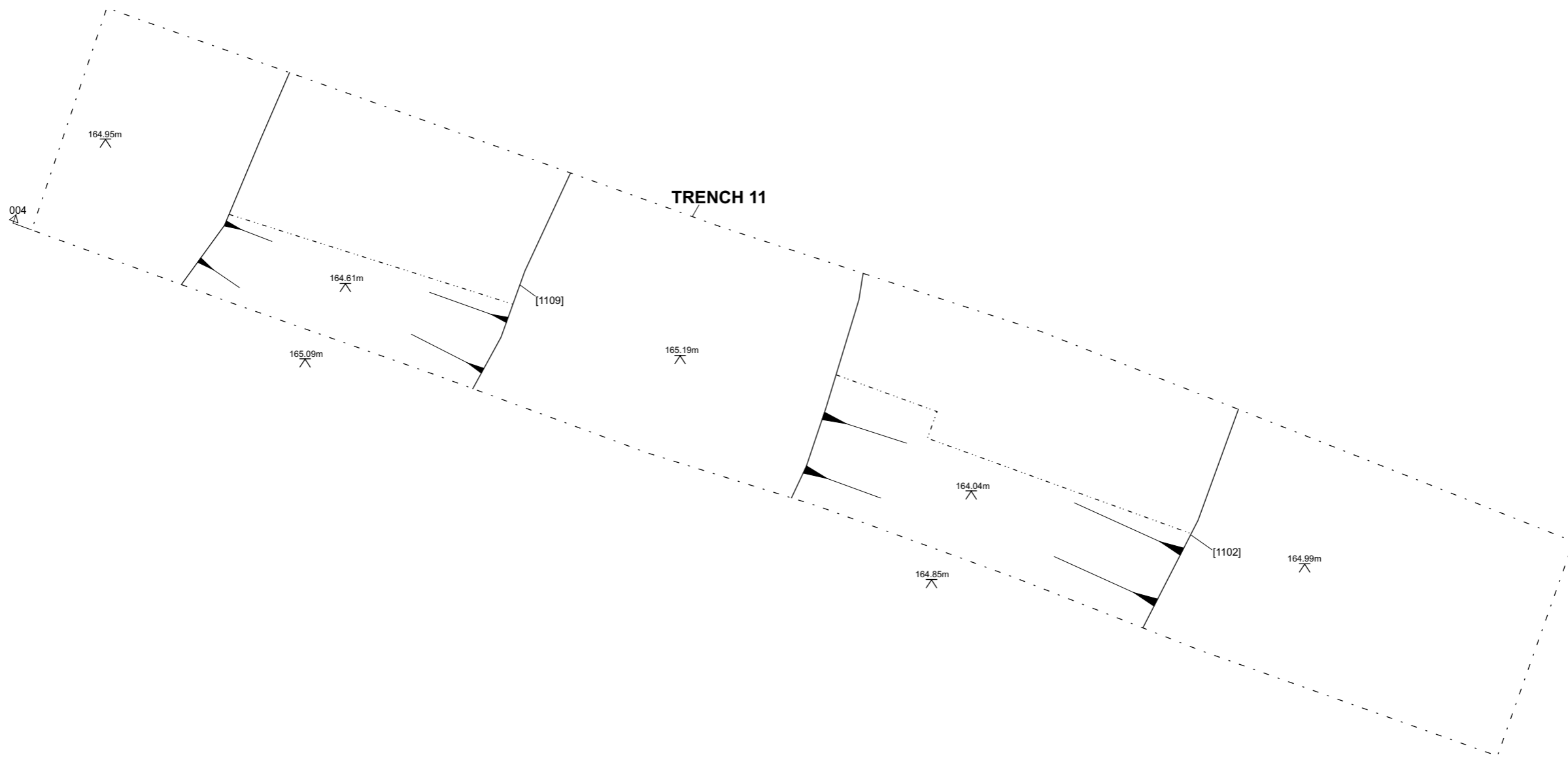


Site Code: VQE19
Accession Code:

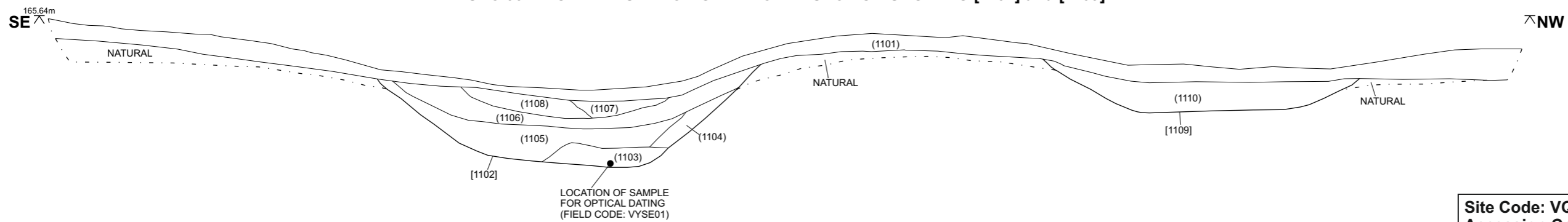
N


0m 20m
1:500

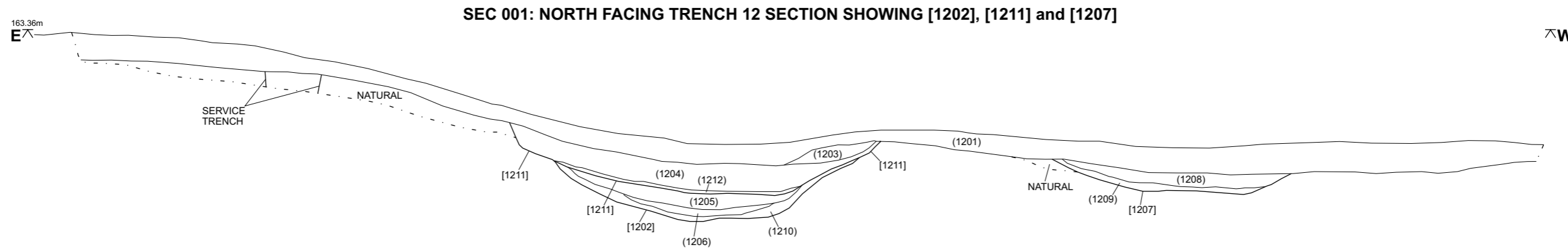
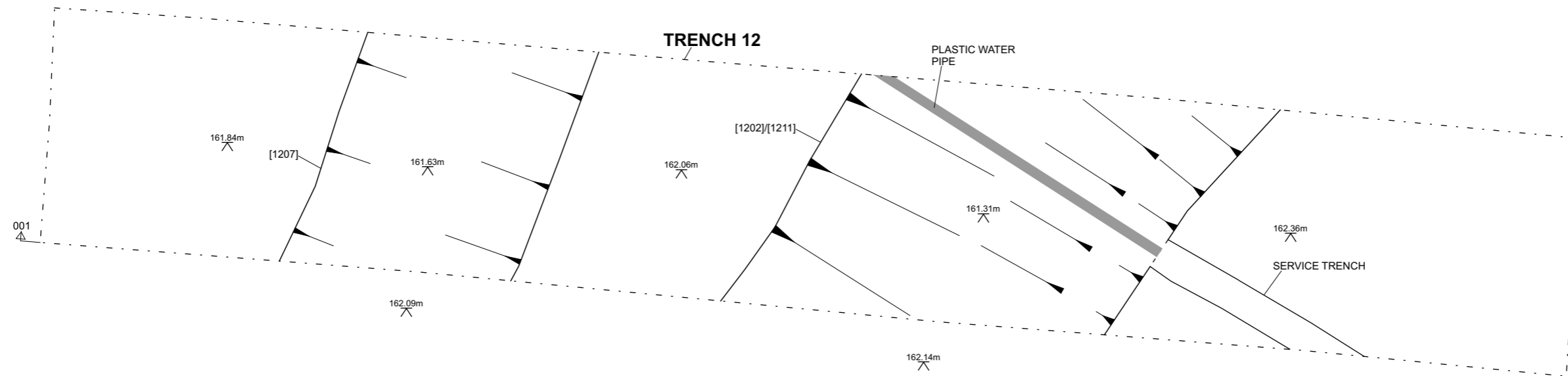
FIGURE 3: Excavated Features in Relation to Earthwork



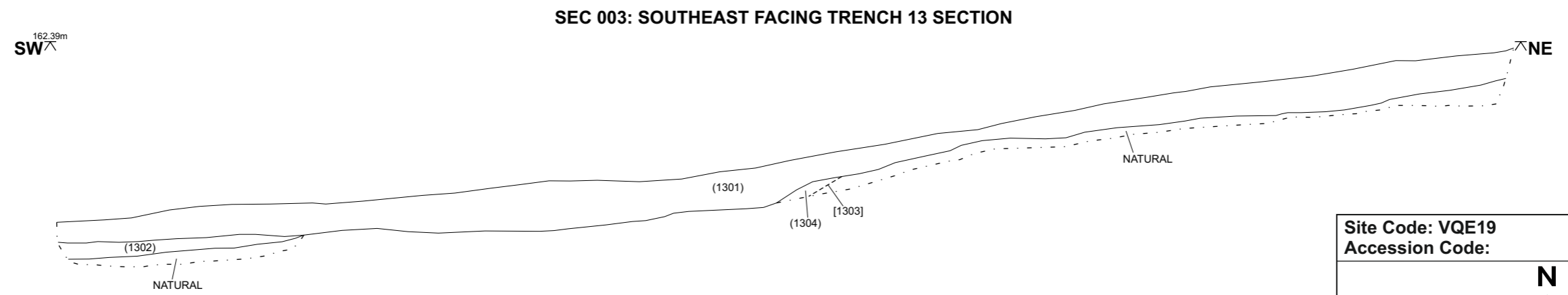
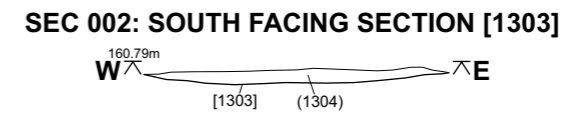
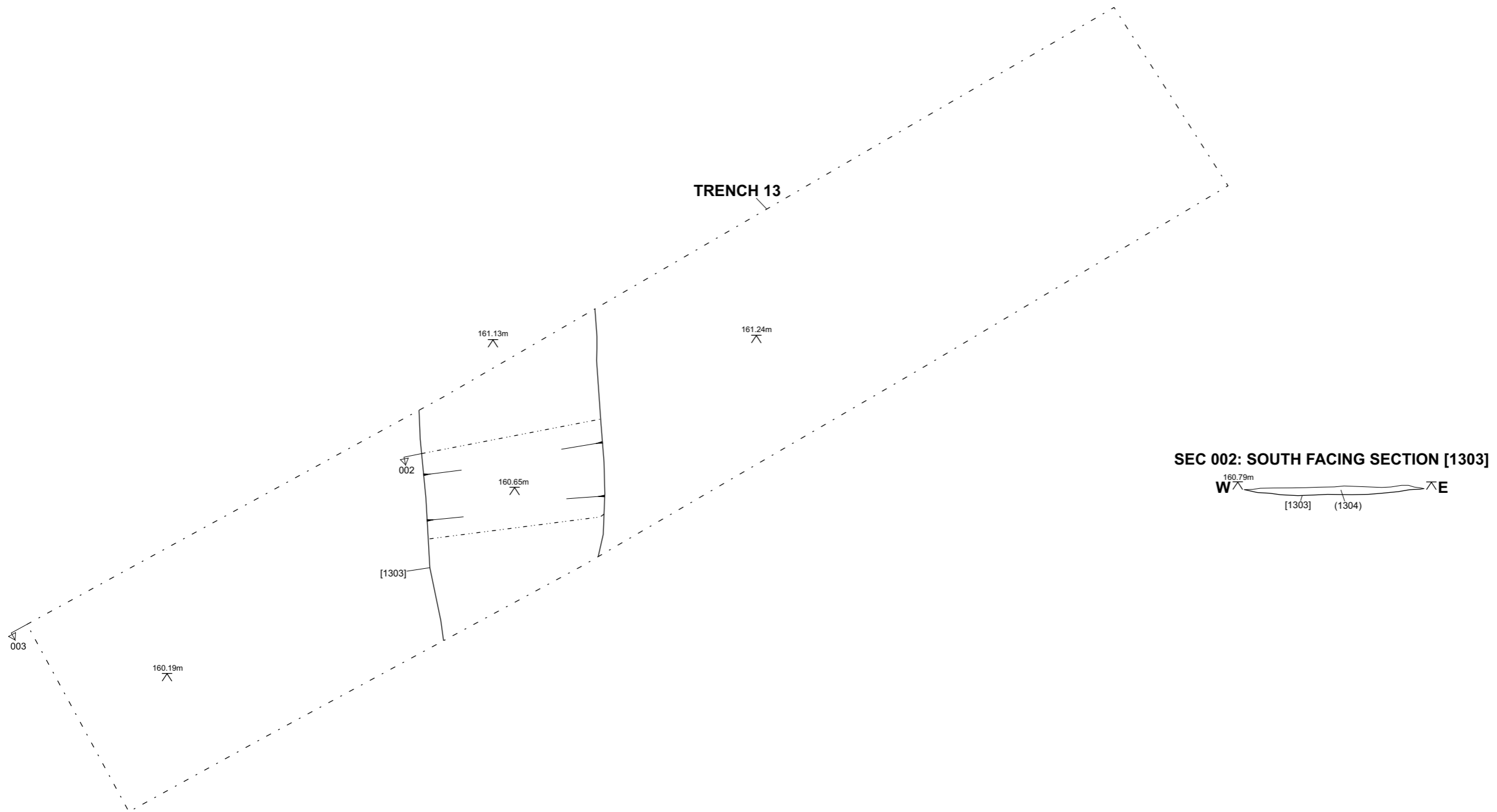
SEC 004: NORTHEAST FACING TRENCH 11 SECTION SHOWING [1102] and [1109]



| |
|--|
| <p>Site Code: VQE19 Accession Code:</p> |
| <p style="text-align: center;">N</p>  <p style="text-align: center;">0m 2m</p> |
| <p>FIGURE 4: Trench 11 Plan and Section</p> |



| |
|---|
| Site Code: VQE19 |
| Accession Code: |
| |
| FIGURE 5: Trench 12 Plan and Section |



| |
|--|
| Site Code: VQE19 |
| Accession Code: |
| |
| |
| FIGURE 6: Trench 13 Plan and Sections |

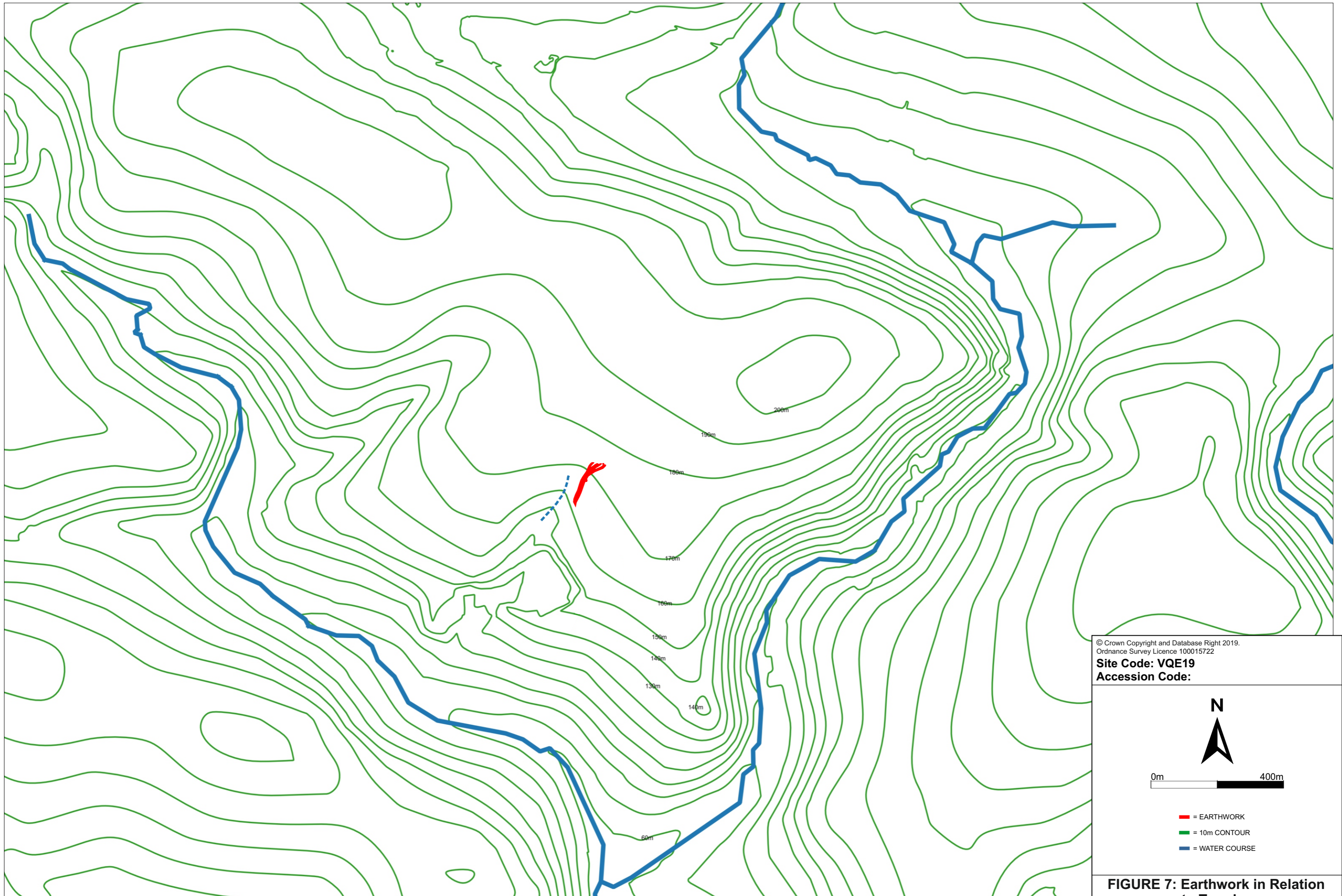
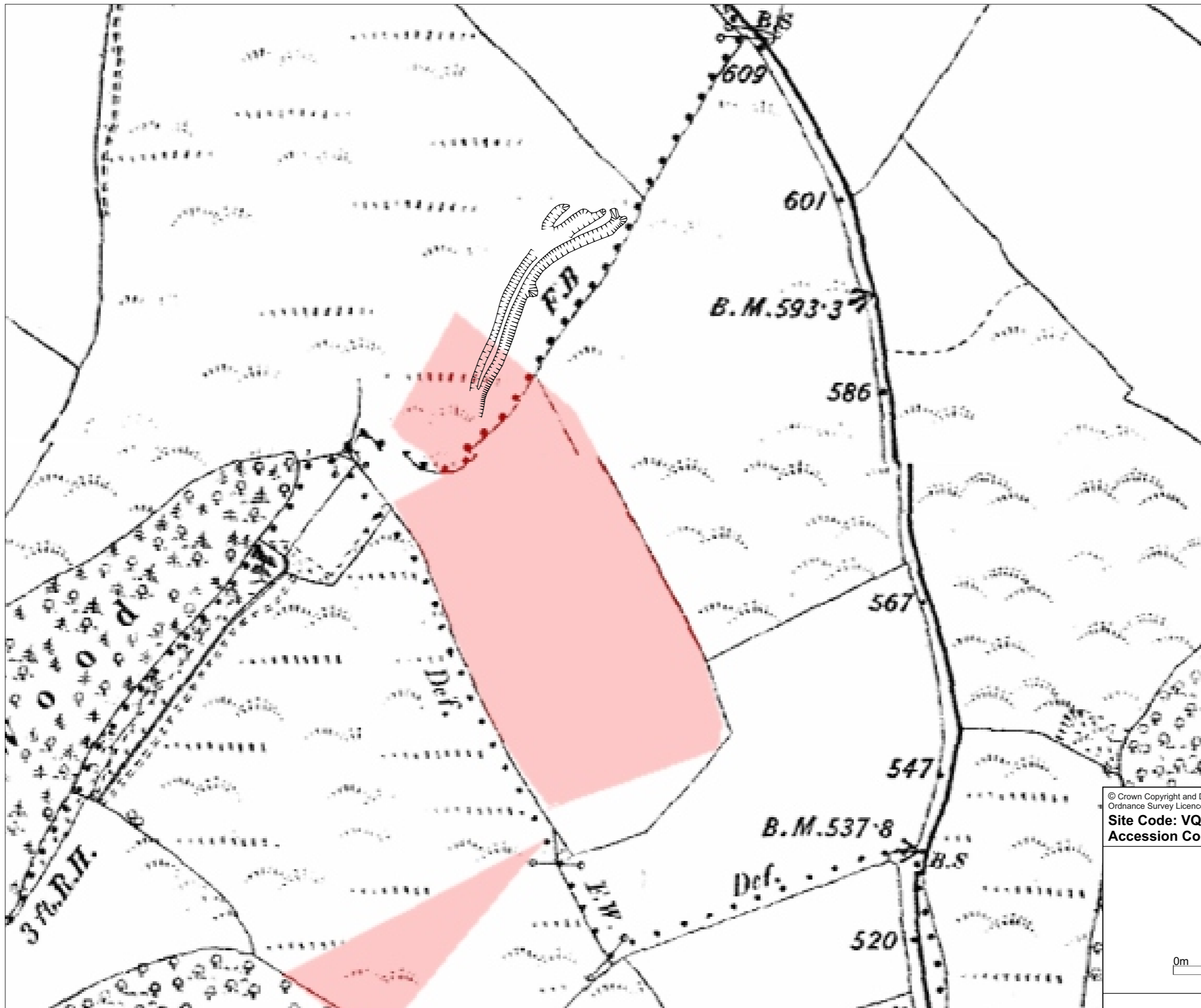


FIGURE 7: Earthwork in Relation to Terrain



© Crown Copyright and Database Right 2019.
Ordnance Survey Licence 100015722

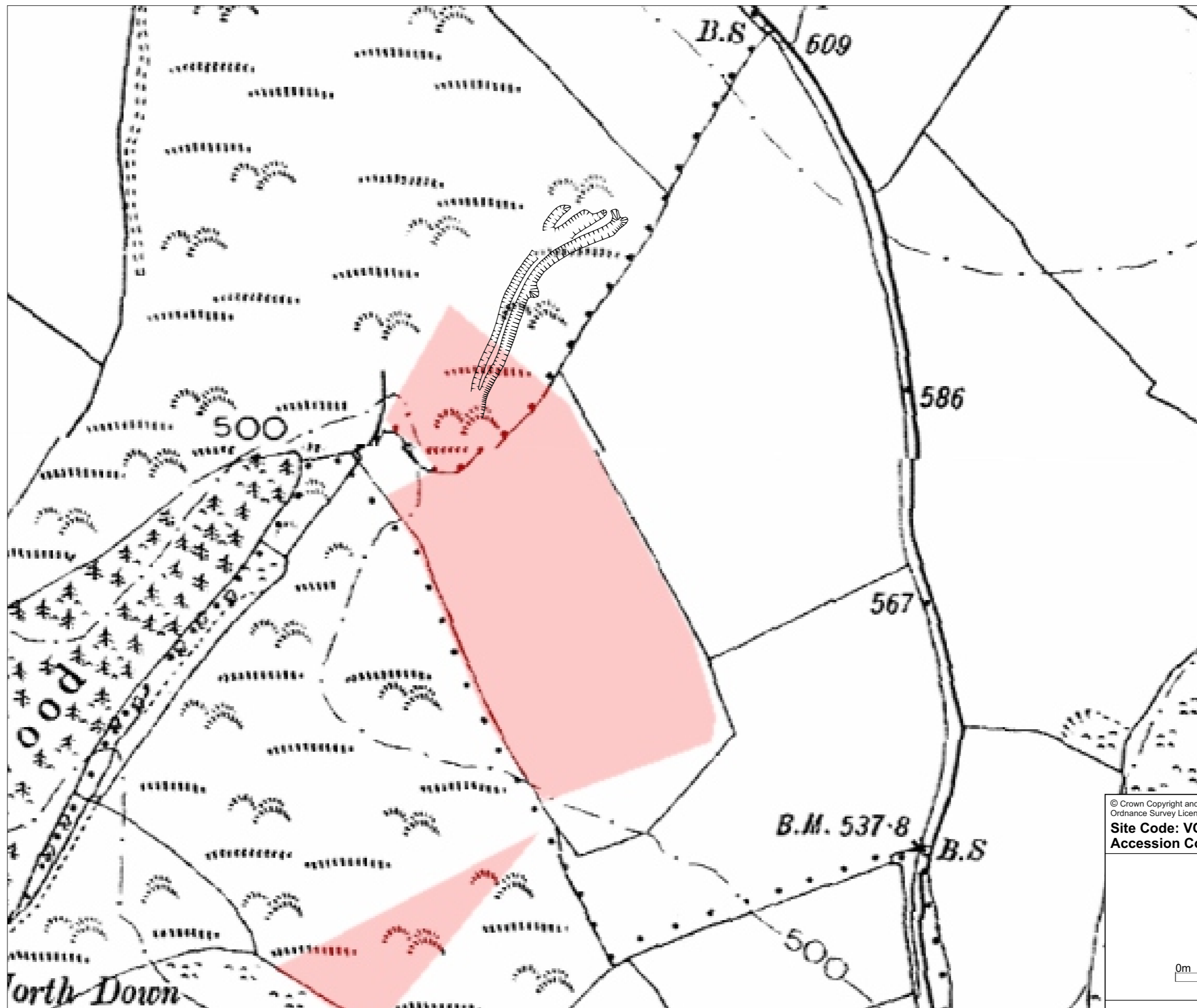
Site Code: VQE19

Accession Code:



0m 100m

FIGURE 8: Earthwork in Relation to 1888 OS Map



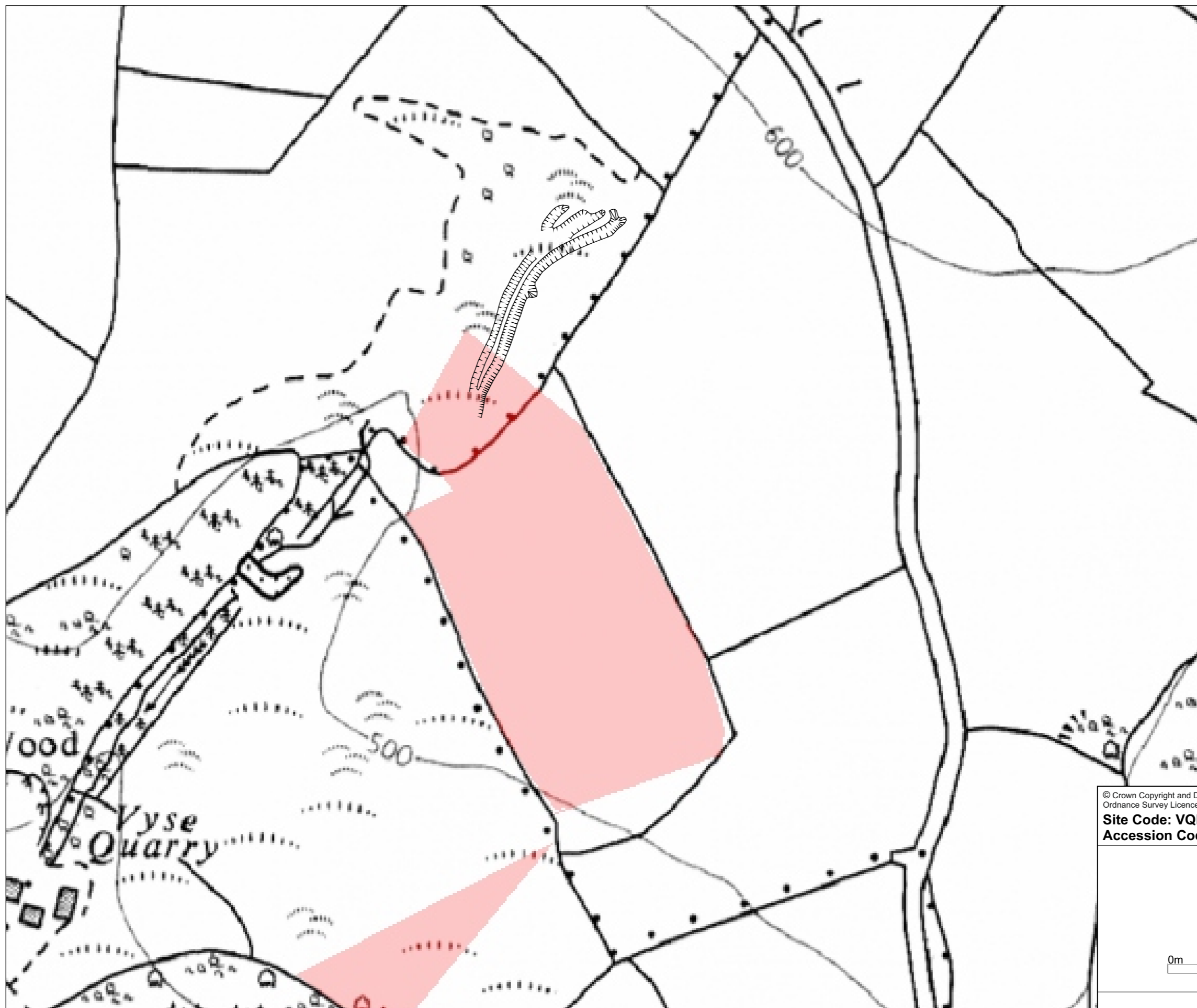
© Crown Copyright and Database Right 2019.
Ordnance Survey Licence 100015722

Site Code: VQE19
Accession Code:



0m 100m

FIGURE 9: Earthwork in Relation to 1905 OS Map



© Crown Copyright and Database Right 2019.
Ordnance Survey Licence 100015722
Site Code: VQE19
Accession Code:

N

0m 100m

FIGURE 10: Earthwork in Relation to 1963 OS Map



PHOTOGRAPH 1: TRENCH 11 LOOKING SOUTHWEST



PHOTOGRAPH 2: TRENCH 12 LOOKING SOUTHWEST



PHOTOGRAPH 3: TRENCH 13, SECTIONS 002 and 003

Site Code: VQE19
Accession Code:

FIGURE 11: Photographs